

# Phospholipase C $\gamma$ 2 is required for basal but not oestrogen deficiency–induced bone resorption

Zsuzsanna Kertész<sup>\*</sup>, Dávid Gyóri<sup>\*</sup>, Szandra Körmendi<sup>†</sup>, Tünde Fekete<sup>‡</sup>, Katalin Kis-Tóth<sup>‡</sup>, Zoltán Jakus<sup>\*</sup>, Georg Schett<sup>§</sup>, Éva Rajnavölgyi<sup>‡</sup>, Csaba Dobó-Nagy<sup>†</sup> and Attila Mócsai<sup>\*</sup>

<sup>\*</sup>Department of Physiology, Semmelweis University School of Medicine, Budapest, Hungary, <sup>†</sup>Independent Section of Radiology, Semmelweis University, Budapest, Hungary, <sup>‡</sup>Department of Immunology, Medical and Health Science Center, University of Debrecen, Debrecen, Hungary, <sup>§</sup>Department of Internal Medicine 3, University of Erlangen-Nuremberg, Erlangen, Germany

## ABSTRACT

**Background** Osteoclasts play a critical role in bone resorption under basal conditions, but they also contribute to pathological bone loss during diseases including postmenopausal osteoporosis. Phospholipase C $\gamma$ 2 (PLC $\gamma$ 2) is an important signalling molecule in diverse haematopoietic lineages. Here, we tested the role of PLC $\gamma$ 2 in basal and ovariectomy-induced bone resorption, as well as in *in vitro* osteoclast cultures using PLC $\gamma$ 2-deficient (PLC $\gamma$ 2<sup>-/-</sup>) mice.

**Materials and methods** The trabecular architecture of long bone metaphyses was tested by micro-CT and histomorphometric analyses. Postmenopausal osteoporosis was modelled by surgical ovariectomy. Osteoclast development and function, gene expression and PLC $\gamma$ 2 phosphorylation were tested on *in vitro* osteoclast and macrophage cultures.

**Results** PLC $\gamma$ 2<sup>-/-</sup> mice had significantly higher trabecular bone mass under basal conditions than wild-type mice. PLC $\gamma$ 2 was required for *in vitro* development and resorptive function of osteoclasts, but not for upregulation of osteoclast-specific gene expression. PLC $\gamma$ 2 was phosphorylated in a Src-family-dependent manner upon macrophage adhesion but not upon stimulation by M-CSF or RANKL. Surprisingly, ovariectomy-induced bone resorption in PLC $\gamma$ 2<sup>-/-</sup> mice was similar to, or even more robust than, that in wild-type animals.

**Conclusions** Our results indicate that PLC $\gamma$ 2 participates in bone resorption under basal conditions, likely because of its role in adhesion receptor signalling during osteoclast development. In contrast, PLC $\gamma$ 2 does not appear to play a major role in ovariectomy-induced bone loss. These results suggest that basal and oestrogen deficiency–induced bone resorption utilizes different signalling pathways and that PLC $\gamma$ 2 may not be a suitable therapeutic target in postmenopausal osteoporosis.

**Keywords** Gene expression, knockout mice, osteoclasts, osteoporosis, phospholipase C $\gamma$ 2, signalling.

Eur J Clin Invest 2012; 42 (1): 49–60

## Introduction

While osteoclasts are important for normal bone turnover, they also contribute to pathological bone loss during osteoporosis, rheumatoid arthritis or osteolytic bone metastases [1–3]. However, it is incompletely understood how osteoclasts contribute to normal and pathological bone resorption and whether they utilize similar intracellular signalling machineries during the two processes.

Osteoclasts are highly specialized phagocytic cells of haematopoietic origin [4]. They develop by an initial macrophage-like differentiation, followed by reprogramming to the osteoclast lineage and fusion of preosteoclasts to mature multinucleated osteoclasts [1,4]. These processes are directed by the M-CSF and the osteoblast-derived RANK ligand (RANKL) cytokines.

A number of recent studies have indicated similar components of osteoclast biology and immune mechanisms, leading to the emergence of the new field of osteoimmunology [5]. Those similarities include activation by closely related cytokines [5–7], shared use of transcription factors [5,8,9] and the

role of immunoreceptor-like signalling pathways (such as Syk activation by immunoreceptor-associated adapters) in osteoclast development [10–14]. The similarity between bone and immune cells is further supported by the similar components used by neutrophil, macrophage and osteoclast signalling and *in vivo* inflammatory processes [15–19].

Phospholipase C $\gamma$  (PLC $\gamma$ ) proteins link tyrosine kinase-coupled receptors to Ca<sup>2+</sup> signalling and PKC activation [20]. While the PLC $\gamma$ 1 isoform is ubiquitously expressed and is required for embryonic development [21,22], PLC $\gamma$ 2 is primarily present in haematopoietic lineage cells and its absence triggers defects in haematopoietic lineage cells [23–28]. Most of those phenotypes are also shared with Syk<sup>-/-</sup> mice or mice with genetic defects of immunoreceptor signalling molecules [15,19,29,30].

PLC $\gamma$ 2 is also activated downstream of the immunoreceptor signalling adapters DAP12 and the Fc-receptor  $\gamma$ -chain (FcR $\gamma$ ) in osteoclast precursors while the downstream activation of the NFATc1 transcription factor is mediated by Ca<sup>2+</sup> signalling through tyrosine phosphorylation pathways [11,31]. The overall similarity between immunoreceptor and PLC $\gamma$ 2-mediated signalling pathways suggests a possible role for PLC $\gamma$ 2 in osteoclast biology.

The above results prompted us to test the role of PLC $\gamma$ 2 in osteoclast development and function, as well as in *in vivo* bone homeostasis under normal and pathological conditions. Our results indicate that PLC $\gamma$ 2 plays an important role in basal bone resorption, likely due to its role in later phases of osteoclast development. Surprisingly, however, PLC $\gamma$ 2 does not play a major role in ovariectomy-induced bone loss.

## Materials and methods

### Animals

Heterozygous mice carrying a deleted allele of the PLC $\gamma$ 2-encoding gene (*Plcg2*<sup>tm1Jni</sup>, referred to as PLC $\gamma$ 2<sup>-/-</sup>) [23] were obtained from James N. Ihle (St. Jude Children's Research Hospital, Memphis, TN, USA) and has been backcrossed to the C57BL/6 genetic background for more than 10 generations. Because of the limited fertility of homozygous PLC $\gamma$ 2<sup>-/-</sup> mice, the mutation was maintained in heterozygous form as described [26].

For *in vivo* experiments, PLC $\gamma$ 2<sup>+/+</sup> or PLC $\gamma$ 2<sup>+/-</sup> mice of identical age and sex (mostly littermates) from the same colony were used as controls. For *in vitro* experiments, either PLC $\gamma$ 2-sufficient mice from the PLC $\gamma$ 2 breeding colony or C57BL/6 mice purchased from the Hungarian National Institute of Oncology (Budapest, Hungary) were used as controls. Because of the limited availability of PLC $\gamma$ 2<sup>-/-</sup> animals, some of the *in vitro* experiments were performed on cells from PLC $\gamma$ 2<sup>-/-</sup> (and appropriate control) bone marrow chimeras generated and tested as described [26]. No difference between the different

sources of mice or bone marrow cells has been observed (not shown).

Mice were kept in individually sterile ventilated cages (Tecniplast, Buguggiate, Italy) in a conventional facility. All animal experiments were approved by the Semmelweis University Animal Experimentation Review Board.

### Ovariectomy

To test oestrogen deficiency-induced bone loss, wild-type and PLC $\gamma$ 2<sup>-/-</sup> females at 8 weeks of age were anesthetized with ketamine and medetomidine and subjected to surgical ovariectomy or sham operation. Six weeks after the operation, the mice were sacrificed and their femurs or tibias were analysed.

### Micro-CT and histomorphometry

Bone architecture under basal conditions was tested on age-matched wild-type and PLC $\gamma$ 2<sup>-/-</sup> male mice at 8–10 weeks of age. Ovariectomy-induced bone loss was tested at 14 weeks of age on wild-type and PLC $\gamma$ 2<sup>-/-</sup> females.

Micro-CT studies were performed on the distal metaphysis of the femurs stored in PBS containing 0.1% Na-azide. Samples were scanned on a SkyScan 1172 (SkyScan, Kontich, Belgium) micro-CT apparatus using a 50 kV and 200  $\mu$ A X-ray source with 0.5-mm aluminium filter, and a rotation step of 0.5° with frame averaging turned on, resulting in an isometric voxel size of 4.5  $\mu$ m. Three-dimensional images were reconstituted and analysed using the NRecon and CT-Analyser software (both from SkyScan). For quantitative analysis, 400 horizontal sections starting 50 sections above the distal growth plate were selected, and the boundaries of trabecular area were selected manually a few voxels away from the endocortical surface [32]. The density threshold for bone tissue was set manually by an experienced investigator. For graphical presentation, the two-dimensional representation of a horizontal section 250 sections above the distal growth plate, as well as the three-dimensional reconstitution of an axial cylinder of 700  $\mu$ m diameter, expanding from 150 to 450 sections above the distal growth plate has been prepared.

Histomorphometry studies were performed on the proximal metaphysis of the tibias. After sacrificing the mice, the bones were placed in 70% ethanol, then fixed overnight in 4% formalin and embedded undecalcified in methylmetacrylate (Technovit; Heraeus Kulzer, Wehrheim, Germany). After polymerization, 3- to 4- $\mu$ m sections were cut with a Jung micrometer (Jung, Heidelberg, Germany) and deplastinated in methoxymethylmetacrylate (Merck, Darmstadt, Germany). Sections were stained with von Kossa and Goldner stains. Bone histomorphometry was performed using a microscope (Nikon, Tokyo, Japan) equipped with a video camera and digital analysis system (OsteoMeasure; OsteoMetrics, Decatur, GA, USA).

Histomorphometry parameters were measured according to international standards [33] as described [34].

### **In vitro cultures, resorption assays and flow cytometry**

Suspensions of bone marrow cells were cultured for 48 h in  $\alpha$ -MEM (Invitrogen, Carlsbad, CA, USA) in the presence of 10 ng/mL recombinant mouse M-CSF (Peprotech, Rocky Hill, NJ, USA). Nonadherent cells (osteoclast/macrophage precursors) were then plated at 0.5 million per cm<sup>2</sup> and cultured in the presence of 20 or 50 ng/mL mouse M-CSF or mouse RANKL (Peprotech) with media changes and replacement of the cytokines every 2–3 days. Cellular morphology and tartrate-resistant acid phosphatase (TRAP) expression were determined after 3–5 days of culture in 24-well tissue culture-treated plates using a commercial TRAP staining kit (Sigma, St. Louis, MO, USA). For *in vitro* resorption assays, osteoclast precursors were plated on BD BioCoat Osteologic slides (BD Biosciences, Bedford, MA, USA), cultured in the presence of M-CSF and RANKL for 10–14 days and processed according to the manufacturer's instructions. Cultures were observed and imaged using a Leica Microsystems (Wetzlar, Germany) DMI6000B inverted microscope. The number of osteoclasts (i.e. TRAP-positive cells with 3 or more nuclei) was counted manually, while the percentage of resorbed area was determined using the IMAGEJ software (NIH, Bethesda, MD, USA).

Macrophages were generated by culturing osteoclast/macrophage precursors in the presence of M-CSF but not RANKL. M-CSF was supplied in the form of purified protein (parallel macrophage and osteoclast studies) or as a 10% conditioned medium from CMG14-12 cells [35] (biochemical studies). Expression of the F4/80 macrophage differentiation antigen was tested as described [19].

### **Analysis of gene expression**

Osteoclast-specific gene expression was tested using quantitative real-time PCR analysis [36] from wild-type or PLC $\gamma$ 2<sup>-/-</sup> cultures generated in the indicated periods of time using the indicated cytokine concentrations. Total RNA was then isolated from the cells with Trizol reagent (Invitrogen). Reverse transcription was performed at 37 °C for 120 min from 100 ng total RNA using the High Capacity cDNA Archive Kit (Applied Biosystems, Foster City, CA, USA). Quantitative real-time PCRs were performed in triplicates with a control reaction containing no reverse transcriptase on an ABI PRISM 7900 (Applied Biosystems) equipment with 40 cycles at 94 °C for 12 s and 60 °C for 60 s using Applied Biosystems Taqman Gene Expression Assay kits. We tested the expression of the mouse *Acp5* (TRAP; Taqman Mm00475698\_m1), *Calcr* (Calcitonin receptor; Mm00432271\_m1), *Ctsk* (cathepsin K; Mm00484039\_m1), *Fos* (c-Fos; Mm00487425\_m1), *Nfatc1*

(NFATc1; Mm00479445\_m1), *Oscar* (OSCAR; Mm00558665\_m1) and *Tm7sf4* (DC-STAMP; Mm04209235\_m1) genes and normalized it to the expression of the housekeeping gene *Gapdh* (GAPDH; Mm99999915\_g1). The comparative C<sub>t</sub> method was used to quantify transcripts.

### **Biochemical and signalling studies**

PLC $\gamma$ 2 expression was determined from Triton X-100-soluble whole osteoclast or macrophage lysates as described [26].

For signalling studies, macrophages were cultured for 5–8 days in bacterial dishes, suspended with 5 mM EDTA and serum starved for 6 h. When indicated, the cells were then incubated with 10  $\mu$ M PP2 (EMD Biosciences, Darmstadt, Germany) for 8 min. The cells were stimulated with 50 ng/mL M-CSF or 50 ng/mL RANKL in suspension or were plated on 6-cm tissue culture-treated dishes. The reaction was stopped after 30 min at 37 °C, and cell lysates were prepared as described [26]. PLC $\gamma$ 2 was precipitated using the Q-20 PLC $\gamma$ 2 antibody (Santa Cruz Biotechnology, Santa Cruz, CA, USA) and captured using a 1 : 1 mixture of Protein A Sepharose (Zymed, South San Francisco, CA, USA) and Protein G Agarose (Invitrogen). Whole-cell lysates or PLC $\gamma$ 2 immunoprecipitates were immunoblotted with phosphorylation-specific antibodies (from Cell Signaling Technology, Danvers, MA) against PLC $\gamma$ 2 (pTyr 759; #3874), ERK (#9101) or the p38 MAP kinase (#9211); nonphospho-specific antibodies against PLC $\gamma$ 2 (Q-20; Santa Cruz), ERK1/2 (combination of C-16 (ERK1) and C-14 (ERK2) from Santa Cruz), p38 MAP kinase (C-20; Santa Cruz), I $\kappa$ B $\alpha$  (#9242; Cell Signaling) or  $\beta$ -actin (AC-74; Sigma); or antibodies against phosphotyrosine (clone 4G10; Millipore, Billerica, MA, USA). Signal intensity was developed using secondary antibodies and ECL reagents from GE Healthcare (Chalfont St. Giles, UK).

### **Statistical analysis**

Experiments were performed at the indicated times with comparable results. Statistical analyses were performed using Student's unpaired two-population *t*-test with unequal variance or by two-way ANOVA. Analysis of the interaction between the effects of genotypes and surgical treatments was performed using Tukey's post hoc test. *P* values below 0.05 were considered statistically significant.

## **Results**

### **micro-CT and histomorphometric analysis of wild-type and PLC $\gamma$ 2<sup>-/-</sup> animals**

We first analysed the composition of trabecular bone of wild-type and PLC $\gamma$ 2<sup>-/-</sup> male mice using micro-CT analysis of the distal metaphysis of the femurs. Significantly more trabeculae were visible in PLC $\gamma$ 2<sup>-/-</sup> animals than in the wild-type mice

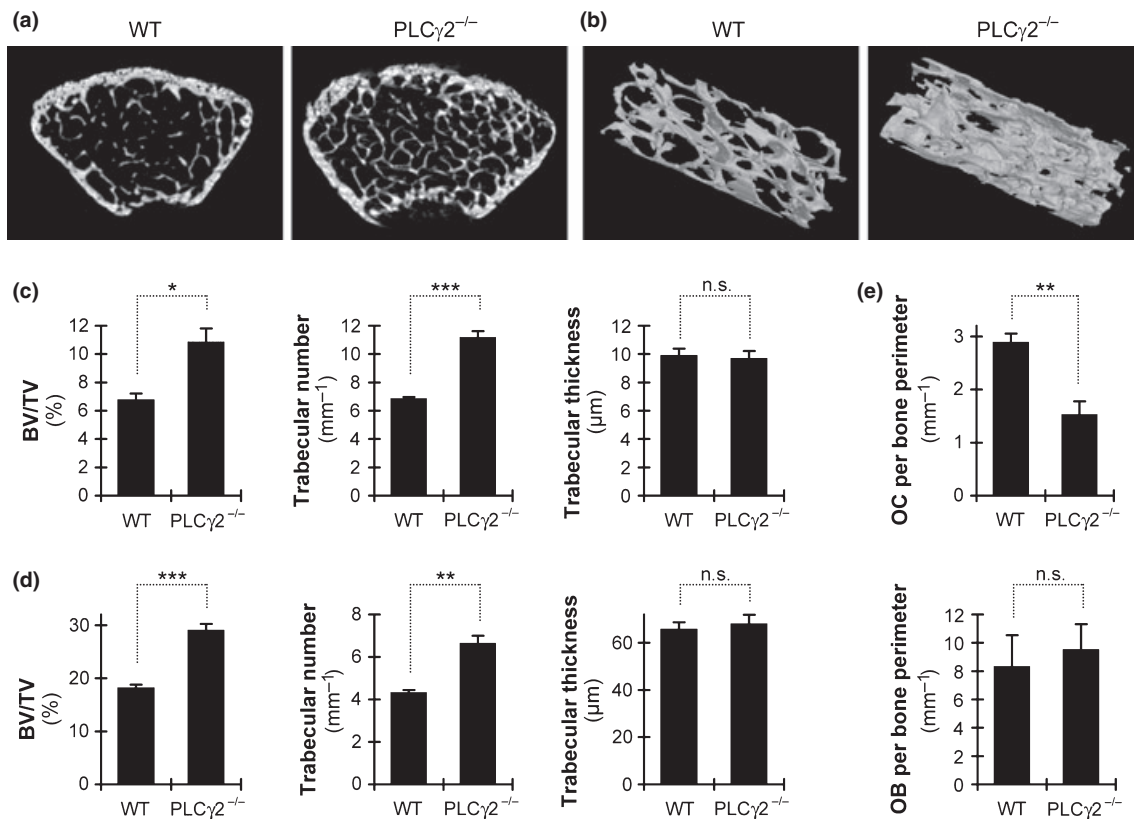


**Figure 1** Micro-CT and histomorphometric analysis of intact PLC $\gamma$ 2<sup>-/-</sup> mice. (a–b) Representative micro-CT sections (a) and three-dimensional reconstitution (b) of the trabecular area of the distal femoral metaphysis of age-matched wild-type (WT) and PLC $\gamma$ 2<sup>-/-</sup> male mice. Distal regions are shown to the lower right in panel b. (c,d) Quantitative micro-CT (c) and histomorphometric (d) analysis of the trabecular bone architecture. (e) Histomorphometric analysis of the number of osteoclasts (OC) or osteoblasts (OB) attached to the trabecular bone surface. Data were obtained from five (a–c) or four (d,e) mice per group at 8–10 weeks of age. The analyses were performed on the distal metaphysis of the femurs (a–c) or the proximal metaphysis of the tibias (d,e). Error bars represent SEM. \* $P < 0.05$ ; \*\* $P < 0.01$ ; \*\*\* $P < 0.002$ ; n.s., not significant; BV/TV, per cent bone volume (bone volume/total volume).

both in raw micro-CT slices (Fig. 1a) and in three-dimensional reconstitution images of an axial cylindrical region (Fig. 1b). Quantification of the entire three-dimensional reconstitution image (Fig. 1c) revealed a significant increase in the per cent bone volume (BV/TV) of PLC $\gamma$ 2<sup>-/-</sup> animals ( $P = 0.011$ ;  $n = 5$ ), which was primarily because of increased trabecular number rather than increased thickness of the individual trabeculae (Fig. 1c).

We also performed histomorphometric analysis of the trabecular bone of the proximal tibia of male mice. Those studies confirmed an increased relative bone volume (BV/TV;  $P = 0.0012$ ;  $n = 4$ ) and trabecular number, but not trabecular thickness is PLC $\gamma$ 2<sup>-/-</sup> animals (Fig. 1d). In addition, a significantly lower number of osteoclasts was seen in PLC $\gamma$ 2<sup>-/-</sup> bones while the number of osteoblasts was not affected (Fig. 1e). Taken

together, PLC $\gamma$ 2<sup>-/-</sup> animals have increased trabecular bone volume likely due to an osteoclast defect.

### PLC $\gamma$ 2 is required for *in vitro* osteoclast development

To test the role of PLC $\gamma$ 2 in osteoclasts, we have cultured wild-type and PLC $\gamma$ 2<sup>-/-</sup> bone marrow cells under osteoclastogenic conditions *in vitro*. As shown in the TRAP-stained images in Fig. 2a and their quantification in Fig. 2b, 20 ng/mL M-CSF and 20 ng/mL RANKL induced significant osteoclast development from wild-type but not from PLC $\gamma$ 2<sup>-/-</sup> bone marrow cells. This defect could not be overcome by increasing the concentration of M-CSF, RANKL or both to 50 ng/mL (Figs 2a,b). However, both wild-type and PLC $\gamma$ 2<sup>-/-</sup> cultures consistently stained positive for TRAP (Fig. 2c), and the percentage of TRAP-positive cells among all mononuclear cells was very similar in the two

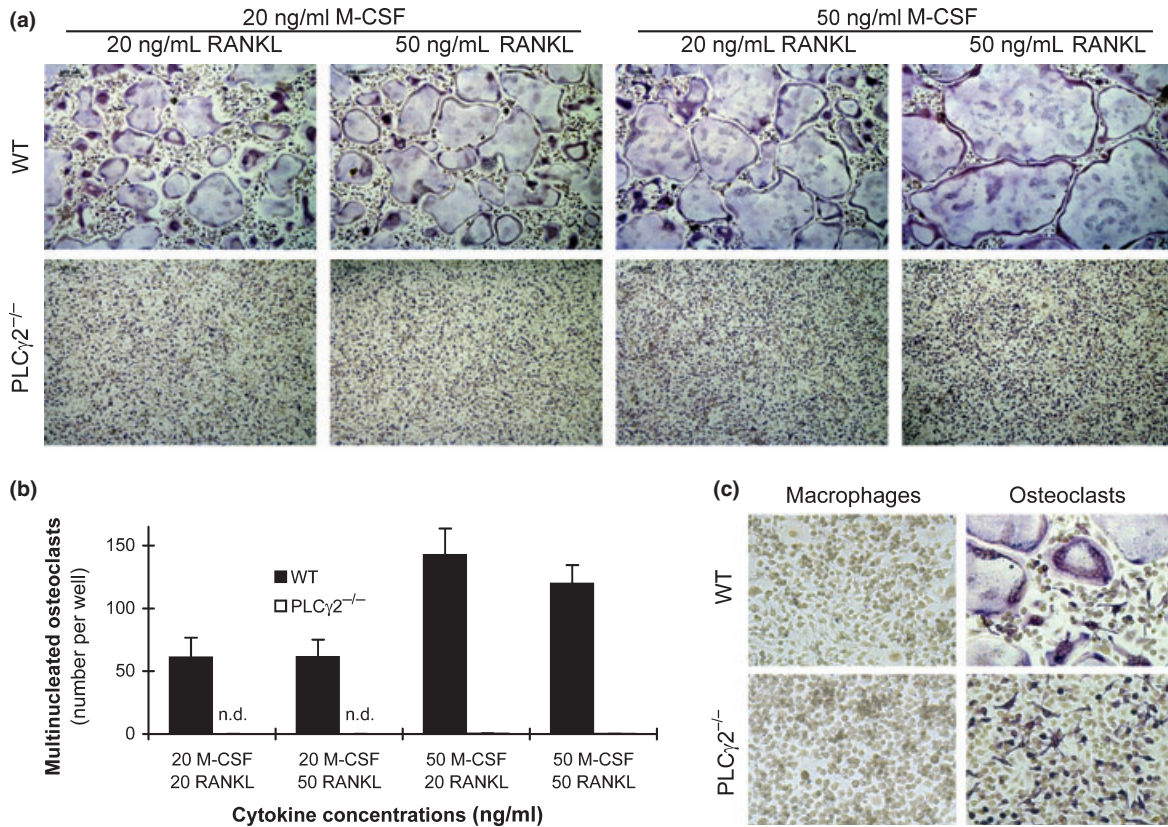


**Figure 2** PLC $\gamma$ 2 is required for *in vitro* osteoclast development. (a) Representative TRAP-stained images of wild-type (WT) and PLC $\gamma$ 2<sup>-/-</sup> bone marrow cells cultured in the presence of the indicated concentrations of recombinant murine M-CSF and RANKL for 4 days. (b) Number of multinucleated osteoclasts (TRAP-positive cells with 3 or more nuclei) in cultures of WT and PLC $\gamma$ 2<sup>-/-</sup> bone marrow cells treated with the indicated concentrations of M-CSF and RANKL for 4 days. (c) Enlarged view of TRAP-stained osteoclast and macrophage cultures generated in the presence of 20 ng/mL M-CSF with (osteoclasts) or without (macrophages) 20 ng/mL RANKL for 4 days. Results were obtained from 15 (a,b) or 7 (c) independent experiments per group. Error bars represent SEM. n. d., not detected.

genotypes (30-35% at 20 ng/mL M-CSF + 20 ng/mL RANKL and 40-45% at 50 ng/mL M-CSF and 50 ng/mL RANKL, irrespective of the genotype of the cells). Taken together, PLC $\gamma$ 2 is required for the *in vitro* development of mature multinucleated osteoclasts in the presence of M-CSF and RANKL but likely not for the initial steps of preosteoclast differentiation.

### PLC $\gamma$ 2 is required for *in vitro* bone resorption

We next tested the effect of PLC $\gamma$ 2 deficiency on osteoclast-mediated bone resorption by culturing bone marrow cells on an artificial hydroxyapatite layer. As shown in Fig. 3, wild-type cells cultured in the presence of 20 ng/mL M-CSF and 20 ng/mL RANKL had a moderate resorptive capacity that was strongly increased by increasing the concentration of both cytokines to 50 ng/mL. In contrast, practically, no resorption could be observed in PLC $\gamma$ 2<sup>-/-</sup> cultures at either cytokine

concentration. Therefore, PLC $\gamma$ 2 is also required for osteoclast-mediated bone resorption, likely reflecting the previously mentioned osteoclast developmental defect (Fig. 2).

### PLC $\gamma$ 2 is not required for macrophage differentiation or expression of osteoclast-specific genes

Our next aim was to address whether PLC $\gamma$ 2 is involved in an earlier or a later phase of osteoclast differentiation. Because we were able to obtain normal numbers of apparently normal macrophages from PLC $\gamma$ 2<sup>-/-</sup> bone marrow cells (Fig. 2c and data not shown) and those macrophages expressed normal levels of the macrophage differentiation marker F4/80 (Fig. 4a), it is unlikely that PLC $\gamma$ 2 is required for the first steps of general myeloid cell differentiation.

We next tested the time course of osteoclast-specific gene expression in *in vitro* cultures by quantitative RT-PCR. As

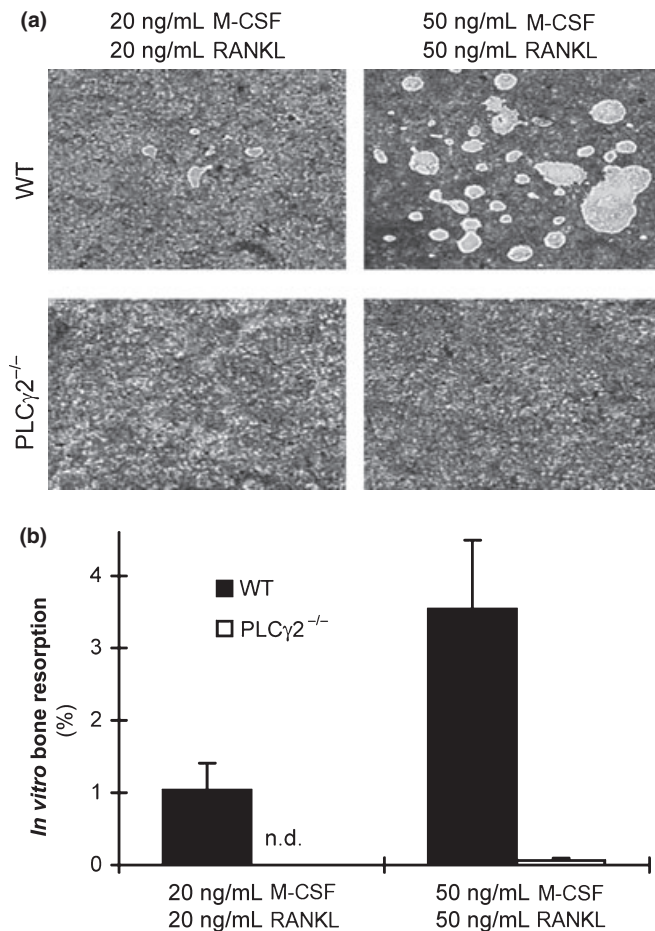


**Figure 3** PLC $\gamma$ 2 is required for *in vitro* resorptive activity of osteoclasts. (a) Representative images of resorption of an artificial hydroxyapatite layer in wild-type (WT) and PLC $\gamma$ 2<sup>-/-</sup> osteoclast cultures. Bone marrow cells were cultured on BD BioCoat Osteologic Plates in the presence of the indicated concentrations of M-CSF and RANKL for 14 days. (b) Quantification of the *in vitro* resorptive activity of WT and PLC $\gamma$ 2<sup>-/-</sup> osteoclast cultures treated with the indicated concentrations of cytokines. Results were obtained from 3 to 7 independent experiments per group. Error bars represent SEM. n.d., not detected.

shown in Fig. 4b, the expression of the *Acp5* (encoding for TRAP), *Calcr* (calcitonin receptor), *Ctsk* (cathepsin K), *Fos* (c-Fos), *Nfatc1* (NFATc1), *Oscar* (OSCAR) and *Tm7sf4* (DC-STAMP) genes was strongly increased during osteoclast differentiation, but none of these genes showed increased expression in parallel macrophage samples. The genetic deficiency of PLC $\gamma$ 2 did not induce any major reduction in osteoclast-specific gene expression, although some partial decrease in expression could be observed, particularly in the case of *Calcr* (Fig. 4b). Most importantly, the expressions of the genes

encoding for the early maturation marker TRAP (*Acp5*), the most plausible PLC $\gamma$ 2 effector NFATc1 (*Nfatc1*) [11,31] and of DC-STAMP (*Tm7sf4*), a critical player of the preosteoclast fusion machinery [37,38], were all upregulated normally in PLC $\gamma$ 2<sup>-/-</sup> cultures (Fig. 4b). These results indicate that PLC $\gamma$ 2 is mostly dispensable for initiation of osteoclast-specific gene expression.

### Biochemical characterization of the PLC $\gamma$ 2-mediated osteoclast signalling pathway

Next, we aimed at the biochemical characterization of PLC $\gamma$ 2 activation in osteoclasts. We first tested the presence of PLC $\gamma$ 2 in parallel macrophage and osteoclast cultures and found that PLC $\gamma$ 2 was expressed at comparable levels in wild-type macrophages and osteoclasts but, as expected, not in PLC $\gamma$ 2<sup>-/-</sup> cells (Fig. 5a).

Osteoclast development is triggered by three major extracellular signals: M-CSF, RANKL and adhesive interactions with the environment (e.g. with tissue culture plastic surface). We next tested which of these three signals trigger PLC $\gamma$ 2 activation, using wild-type macrophages stimulated with M-CSF or RANKL in suspension (which was required to avoid parallel engagement of adhesion receptors), or plated on a tissue culture plastic surface. Both an immunoprecipitation approach followed by immunoblotting with anti-phosphotyrosine antibodies (Fig. 5b) and a direct immunoblotting using phospho-specific PLC $\gamma$ 2 antibodies (Fig. 5c) revealed PLC $\gamma$ 2 phosphorylation upon adhesion of macrophages but not upon M-CSF or RANKL stimulation in suspension. Additional attempts with M-CSF or RANKL stimulation for various periods of time or using various cytokine concentrations ranging from 10 to 100 ng/mL did not reveal a consistent PLC $\gamma$ 2 phosphorylation in suspension either (not shown). On the other hand, M-CSF-induced ERK phosphorylation and RANKL-induced p38 MAP kinase phosphorylation and NF $\kappa$ B activation (degradation of I $\kappa$ B $\alpha$ ) could readily be observed under these conditions (Fig. 5c), indicating intact basic M-CSF and RANKL signalling in suspension. Therefore, PLC $\gamma$ 2 appears to be activated by adhesive interactions rather than by stimulation with M-CSF or RANKL cytokines.

We have also tested the role of Src-family kinases in PLC $\gamma$ 2 phosphorylation. As shown in Fig. 5d, pretreatment of macrophages with the Src-family inhibitor PP2 completely abrogated the PLC $\gamma$ 2 phosphorylation response, indicating that the adhesion-induced PLC $\gamma$ 2 activation requires members of the Src kinase family.

### PLC $\gamma$ 2<sup>-/-</sup> mice show normal ovariectomy-induced bone resorption

Because osteoclast-mediated bone resorption contributes to postmenopausal osteoporosis [39], we hypothesized that PLC $\gamma$ 2

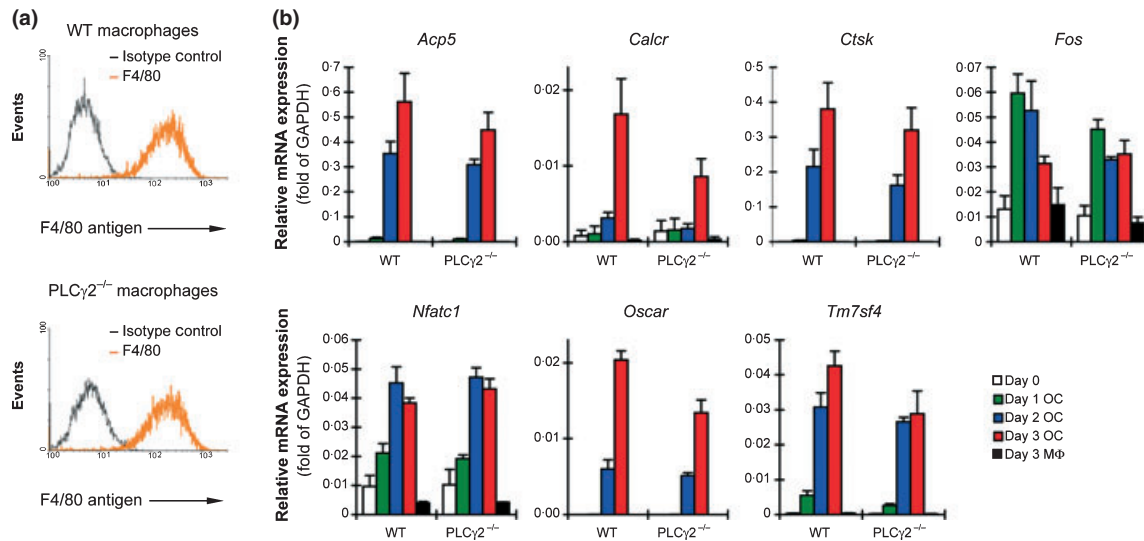


**Figure 4** Normal macrophage development and osteoclast-specific gene expression. (a) Flow cytometric analysis of the expression of the F4/80 macrophage differentiation marker on wild-type (WT) and PLC $\gamma$ 2<sup>-/-</sup> macrophages generated by culturing bone marrow cells in the presence of recombinant murine M-CSF. Curves of isotype control-stained cells show non-specific labelling. (b) Analysis of the expression of osteoclast-specific genes in WT and PLC $\gamma$ 2<sup>-/-</sup> osteoclast (OC) and macrophage (M $\Phi$ ) cultures. WT and PLC $\gamma$ 2<sup>-/-</sup> bone marrow cells were cultured in the presence of 50 ng/mL with (OC) or without (M $\Phi$ ) 50 ng/mL RANKL for the indicated period of time, and then the expression of the *Acp5* (TRAP), *Calcr* (Calcitonin receptor), *Ctsk* (Cathepsin K), *Fos* (c-Fos), *Nfatc1* (NFATc1), *Oscar* (OSCAR) and *Tm7sf4* (DC-STAMP) genes was determined using quantitative RT-PCR. The results shown were obtained from 3 to 6 independent experiments per group. Error bars represent SEM.

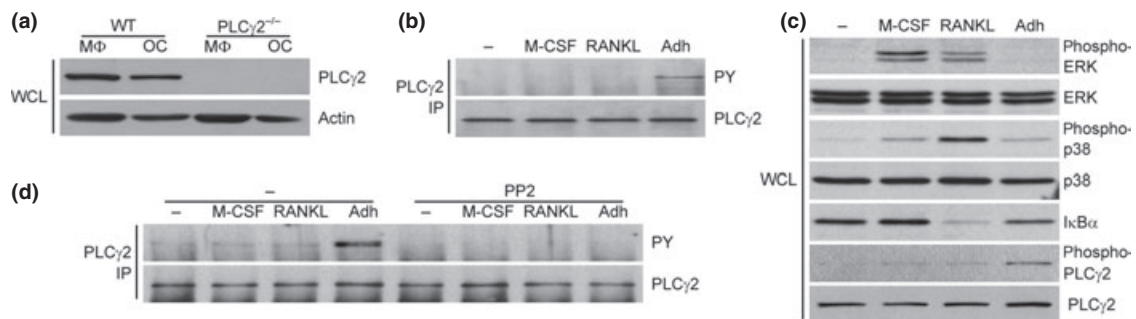


**Figure 5** Cellular adhesion triggers PLC $\gamma$ 2 phosphorylation. (a) Expression of PLC $\gamma$ 2 in macrophages (M $\Phi$ ) and osteoclasts (OC). Wild-type (WT) and PLC $\gamma$ 2<sup>-/-</sup> bone marrow cells were cultured in the presence of 50 ng/mL M-CSF with (OC) or without (M $\Phi$ ) 50 ng/mL RANKL for 4 days, followed by preparation of whole-cell lysates (WCL) and immunoblotting for PLC $\gamma$ 2 and  $\beta$ -actin. B-C, Stimulus-induced phosphorylation of PLC $\gamma$ 2. Wild-type macrophages were treated with 50 ng/mL M-CSF, 50 ng/mL RANKL or kept unstimulated in suspension, or they were plated on tissue culture-treated plastic dishes (Adh). After 30 min of incubation, cell was lysed and processed for immunoprecipitation (IP) of PLC $\gamma$ 2 followed by immunoblotting using anti-phosphotyrosine (PY) antibodies, (b) or WCL were immunoblotted using phosphorylation-specific antibodies against ERK, the p38 MAP kinase (p38) and PLC $\gamma$ 2 or nonphospho-specific antibodies against I $\kappa$ B $\alpha$  (c). Immunoblotting for ERK, p38 and PLC $\gamma$ 2 served as loading control. (d) Role of Src-family kinases in PLC $\gamma$ 2 phosphorylation. Wild-type macrophages were pretreated in the presence or absence of 10  $\mu$ M PP2 and then stimulated and their PLC $\gamma$ 2 phosphorylation tested as in panel b. Results shown represent 3–5 independent experiments with similar results.

may also play a role in oestrogen deficiency-induced bone loss. That possibility was tested by subjecting wild-type and PLC $\gamma$ 2<sup>-/-</sup> animals to surgical ovariectomy, followed by

micro-CT and histomorphometric analysis 6 weeks later. Representative raw micro-CT sections (Fig. 6a), three-dimensional reconstitution images (Fig. 6b) and quantitative micro-CT

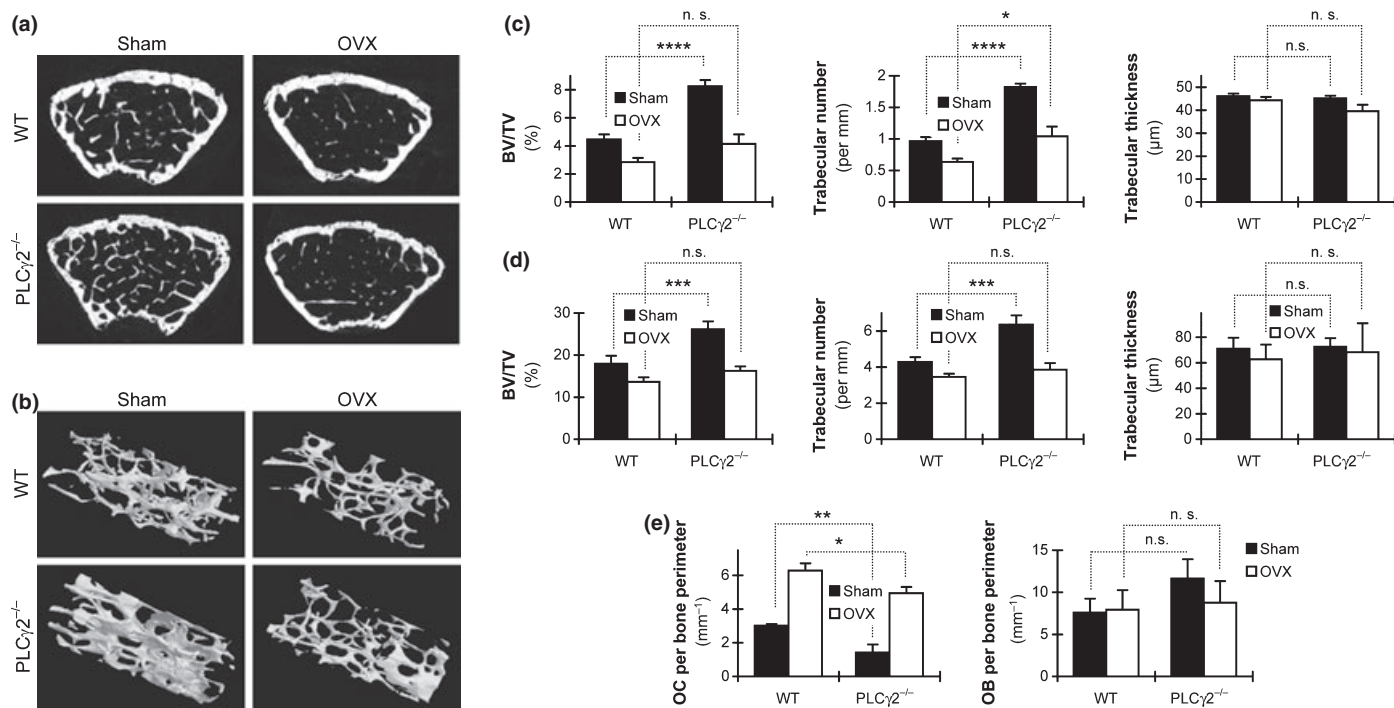


**Figure 6** PLC $\gamma$ 2 is not required for ovariectomy-induced bone resorption. (a,b) Representative micro-CT sections (a) and three-dimensional reconstruction (b) of the trabecular area of the distal metaphysis of the femur of wild-type (WT) and PLC $\gamma$ 2<sup>-/-</sup> female mice subjected to surgical ovariectomy (OVX) or a sham operation. Distal regions are shown to the lower right in panel b. (c,d) Quantitative micro-CT (c) or histomorphometric (d) analysis of the trabecular bone architecture of ovariectomized or sham-operated mice of the indicated genotypes. (e) Histomorphometric analysis of the number of osteoclasts (OC) or osteoblasts (OB) attached to the trabecular bone surface. Data were obtained from 7 (WT) or 4 (PLC $\gamma$ 2<sup>-/-</sup>) mice per group (a-c) or from three mice per group (d,e). Surgical operation was performed at 8 weeks of age followed by an additional 6 weeks before the mice were sacrificed and their bones were removed for analysis. Error bars represent SEM of the indicated number of animals. \* $P < 0.05$ ; \*\* $P < 0.01$ ; \*\*\* $P < 0.002$ ; \*\*\*\* $P < 0.0004$ ; n.s., not significant; BV/TV, per cent bone volume (bone volume/total volume).

analyses (Fig. 6c) indicated that, similar to intact male animals (Fig. 1), sham-operated PLC $\gamma$ 2<sup>-/-</sup> females also had increased trabecular bone density, which was reflected in a nearly two-fold increase in relative bone volume (BV/TV;  $P = 0.00031$ ;  $n = 7$  (wild type) vs. 4 (PLC $\gamma$ 2<sup>-/-</sup>)). As expected, surgical ovariectomy led to a significant reduction in the per cent bone volume (BV/TV) of wild-type mice ( $P = 0.025$ ;  $n = 7$ ). Contrary to our expectations, however, the per cent bone volume of PLC $\gamma$ 2<sup>-/-</sup> animals was also significantly reduced ( $P = 0.00023$ ;  $n = 4$ ) and that reduction was even higher in PLC $\gamma$ 2<sup>-/-</sup> mice than in wild-type animals both in terms of absolute reduction in BV/TV values (4.1 vs. 1.6 percentage points, respectively) and in percentage of the BV/TV values of the sham-operated control animals (50% vs. 36%, respectively). The difference of the effect of ovariectomy on wild-type and PLC $\gamma$ 2<sup>-/-</sup> animals (interaction of the genotypes and surgical procedures) proved to be statistically significant ( $P = 0.0090$ ). Importantly, while the

BV/TV values of sham-operated wild-type and PLC $\gamma$ 2<sup>-/-</sup> animals were statistically highly significant ( $P = 0.00025$ ), there was no significant difference between the two genotypes after the ovariectomy procedure ( $P = 0.25$ ;  $n = 7$  (wild type) vs. 4 (PLC $\gamma$ 2<sup>-/-</sup>)). Similar differences could be observed in the trabecular numbers, whereas the trabecular thickness remained unaffected by the different genotypes and surgical procedures (Fig. 6c).

The above-mentioned findings were also confirmed by histomorphometric analysis of ovariectomy-induced bone loss in the proximal tibia. As shown in Fig. 6d, that analysis confirmed the increased per cent bone volume (BV/TV) in sham-operated PLC $\gamma$ 2<sup>-/-</sup> animals ( $P = 0.0010$ ;  $n = 3$ ) and a reduction in per cent bone volume in ovariectomized wild-type mice ( $P = 0.038$ ;  $n = 3$ ). Importantly, the ovariectomy procedure induced a significantly more pronounced reduction in per cent bone volume in PLC $\gamma$ 2<sup>-/-</sup> mice than in wild-type animals, both

in terms of absolute reduction in BV/TV values (9.9 vs. 4.3 percentage points, respectively) and in per cent of the BV/TV values of the sham-operated control animals (38% vs. 24%, respectively). The difference of the effect of ovariectomy on wild-type and PLC $\gamma$ 2<sup>-/-</sup> animals (interaction of the genotypes and surgical procedures) proved again to be statistically significant ( $P = 0.013$ ). Similar to the micro-CT data (Fig. 6a), while the BV/TV values of sham-operated wild-type and PLC $\gamma$ 2<sup>-/-</sup> animals were statistically highly significant ( $P = 0.0010$ ), that difference faded away after the ovariectomy procedure ( $P = 0.24$ ;  $n = 3$ ). A similar picture was seen during the analysis of trabecular numbers, whereas the trabecular thickness remained unaffected by the different genotypes and surgical procedures (Fig. 6d).

Additional studies testing the number of osteoclasts and osteoblasts attached to the bone surface indicated that although the number of osteoclasts was significantly lower in the sham-operated PLC $\gamma$ 2<sup>-/-</sup> mice than in the wild-type ones ( $3.0 \pm 0.1$  vs.  $1.4 \pm 0.5$  per mm, respectively;  $P = 0.0036$ ;  $n = 3$ ), the number of osteoclasts was strongly increased and reached a comparable, though, still significantly different level ( $6.3 \pm 0.4$  vs.  $5.0 \pm 0.4$  per mm, respectively;  $P = 0.010$ ;  $n = 3$ ) in the two genotypes after the ovariectomy procedure (Fig. 6e). The difference of the effect of ovariectomy on wild-type and PLC $\gamma$ 2<sup>-/-</sup> animals (interaction of the genotypes and surgical procedures) did not prove to be statistically significant ( $P = 0.56$ ;  $n = 3$ ), indicating that PLC $\gamma$ 2<sup>-/-</sup> animals were able to upregulate osteoclast numbers upon oestrogen deficiency normally. Analysis of the number of osteoblasts did not find any significant difference between any of the groups tested (Fig. 6e).

Taken together, these results suggest that ovariectomized PLC $\gamma$ 2<sup>-/-</sup> animals are capable of reducing their bone mass to levels comparable to those seen in similarly treated wild-type animals, likely because of similar oestrogen deficiency-induced increase in osteoclast numbers in the two genotypes.

## Discussion

In the first part of this study, we showed that PLC $\gamma$ 2<sup>-/-</sup> mice have increased basal bone density, likely due to reduced *in vivo* osteoclast number reflecting the role of PLC $\gamma$ 2 in a later phase of osteoclast development. These results raised the possibility that PLC $\gamma$ 2 may also participate in pathological bone resorption, such as oestrogen deficiency-induced osteoporosis. Much to our surprise, however, PLC $\gamma$ 2<sup>-/-</sup> mice showed similar, or even more pronounced, ovariectomy-induced bone resorption than their wild-type counterparts. Therefore, PLC $\gamma$ 2 does not appear to be required for oestrogen deficiency-induced bone loss.

The experiments presented in this paper (part of which were published in an abstract form before [40]) were initiated based on our prior experiments showing defective osteoclast develop-

ment and *in vivo* bone resorption in mice lacking immunoreceptor signalling adapter molecules or the Syk tyrosine kinase [10], as well as the similarity between various Syk<sup>-/-</sup> and PLC $\gamma$ 2<sup>-/-</sup> phenotypes [15,19,23–26,41]. However, two other groups have also independently reported *in vitro* osteoclast development and *in vivo* bone resorption defects in PLC $\gamma$ 2<sup>-/-</sup> mice [42,43]. Although all three reports conclude that PLC $\gamma$ 2 is required for *in vitro* osteoclast development and basal bone resorption *in vivo*, they provide different explanations for those observations. Mao *et al.* [42] and Chen *et al.* [43] reported dramatically reduced expression of osteoclast-specific genes (such as those encoding TRAP, NFATc1, cathepsin K or the calcitonin receptor) in PLC $\gamma$ 2<sup>-/-</sup> cultures, suggesting that PLC $\gamma$ 2 is required for an early step of osteoclast differentiation. A plausible explanation was that a PLC $\gamma$ 2-induced intracellular Ca<sup>2+</sup> signal triggered activation of NFATc1, a Ca<sup>2+</sup>-sensitive master regulator of osteoclast-specific gene expression [31]. Surprisingly, our own more detailed analyses did not reveal any substantial defect of osteoclast-specific gene expression in PLC $\gamma$ 2<sup>-/-</sup> cultures, and the expression of NFATc1 was not at all affected by the PLC $\gamma$ 2 mutation (Fig. 4b). Based on the time course of the expression of those genes and their low expression in parallel macrophage samples (Fig. 4b), it is unlikely that our results are attributed to non-specific amplification artefacts. It is also unlikely that our results are owing to inappropriate selection of the cytokine concentrations used because we did not observe reduced gene expression levels in PLC $\gamma$ 2<sup>-/-</sup> cultures even when the concentration of both M-CSF and RANKL was reduced to 20 ng/mL, whereas the PLC $\gamma$ 2<sup>-/-</sup> mutation caused severe osteoclast developmental defect even when the concentration of both cytokines was increased to 100 ng/mL (not shown). In addition, we consistently observed a large percentage of TRAP-positive mononuclear cells in PLC $\gamma$ 2<sup>-/-</sup> osteoclast cultures (Fig. 2c), and such cells were also present in the PLC $\gamma$ 2<sup>-/-</sup> osteoclast cultures shown by Mao *et al.* [42] and Chen *et al.* [43]. Taken together, osteoclast-specific gene expression is not (or not completely) blocked in PLC $\gamma$ 2<sup>-/-</sup> cultures, necessitating alternative explanations for the PLC $\gamma$ 2<sup>-/-</sup> osteoclast phenotype.

Another possible explanation for the PLC $\gamma$ 2<sup>-/-</sup> osteoclast phenotype could be the participation of PLC $\gamma$ 2 in preosteoclast fusion, a process mediated in part by the DC-STAMP molecule [37,38]. While our gene expression studies (Fig. 4b) did not reveal any major role for PLC $\gamma$ 2 in RANKL-induced upregulation of DC-STAMP, it has yet to be tested whether PLC $\gamma$ 2 is involved in signal transduction by DC-STAMP or another preosteoclast fusion receptor.

Osteoclast development requires a complex interplay between signals from M-CSF, RANKL and ligation of adhesion receptors [44]. Because RANKL stimulation of adherent bone marrow-derived macrophages triggered PLC $\gamma$ 2

phosphorylation, Mao *et al.* [42] and Chen *et al.* [43] suggested that PLC $\gamma$ 2 is activated downstream of RANK. That conclusion, however, is confounded by the ligation of both RANK and adhesion receptors in that assay. In contrast, we did not observe any PLC $\gamma$ 2 phosphorylation upon stimulating wild-type macrophages with RANKL (or M-CSF) in suspension, whereas cellular adhesion consistently triggered robust phosphorylation of the protein in the absence of any cytokines (Fig. 5b,c). These results suggest that PLC $\gamma$ 2 is primarily involved in adhesion receptor rather than in RANK signal transduction, a possibility consistent with the role of PLC $\gamma$ 2 in integrin signalling of neutrophils [24,26] and its proposed modulatory effect on integrin signalling in preosteoclasts [45].

The analysis of ovariectomy-induced bone resorption is likely the most clinically relevant aspect of our study. While the increased basal bone volume (Fig. 1) and the defective *in vitro* osteoclast development and function (Figs 2 and 3) in PLC $\gamma$ 2<sup>-/-</sup> mice suggested a role for PLC $\gamma$ 2 in pathological bone resorption, ovariectomy-induced bone loss in PLC $\gamma$ 2<sup>-/-</sup> mice was unexpectedly normal or even more pronounced than in wild-type animals (Fig. 6). Because this was observed both in the distal femur and in the proximal tibia and by two independent approaches (micro-CT and histomorphometry), we believe that PLC $\gamma$ 2 is not a major general component of oestrogen deficiency-induced bone resorption. However, we cannot exclude the possibility that ovariectomy-induced bone resorption at certain sites or under some specific conditions would be defective in PLC $\gamma$ 2<sup>-/-</sup> animals.

It is at present unclear to us how exactly PLC $\gamma$ 2<sup>-/-</sup> animals are able to reduce their bone mass during oestrogen deficiency. However, the fact that the ovariectomy-induced increase in the number of osteoclasts was similar in the two genotypes despite significantly reduced basal number of osteoclasts in PLC $\gamma$ 2<sup>-/-</sup> mice (Fig. 6e) suggests the existence of PLC $\gamma$ 2-independent mechanisms triggering oestrogen deficiency-induced osteoclast development. Whether those are mediated by cell-cell interactions (e.g. with osteoblasts) not present in the *in vitro* cultures [10,11], by excessive release of cytokines overcoming osteoclast developmental defects [46] or by the amplification of PLC $\gamma$ 2-independent signal transduction pathways, should be the subject of future research.

It has been generally believed that osteoclasts use similar signal transduction pathways during basal and induced (e.g. oestrogen deficiency-induced) bone resorption. Therefore, it has been assumed that the identification of novel osteoclast signalling molecules may provide suitable targets for the therapeutic intervention in pathological bone loss, such as postmenopausal osteoporosis. Our results showing normal ovariectomy-induced bone loss in PLC $\gamma$ 2<sup>-/-</sup> animals indicate that this may not be the case. Interestingly, a prior study showed that ovariectomy-induced bone loss in the highly

osteopetrotic DAP12<sup>-/-</sup>FcR $\gamma$ <sup>-/-</sup> animals is comparable to, or even higher than, that in wild-type mice [47]. All these results suggest differential osteoclast signalling requirements for basal and oestrogen deficiency-induced bone resorption and indicate that care should be taken when extrapolating findings on basal bone resorption to pathological conditions. These results also indicate that limited clinical benefit can be expected from therapeutic targeting of PLC $\gamma$ 2 in postmenopausal osteoporosis.

### Acknowledgements

We thank James Ihle for the PLC $\gamma$ 2<sup>-/-</sup> animals; Zsuzsa Krasznai for help with initial experiments; Edina Simon and Krisztina Makara for technical assistance; Norbert Gyöngyösi for help with statistical analyses. This work was supported by the Wellcome Trust (International Senior Research Fellowship No. 087782 to A. M.), the European Research Council (Starting Independent Investigator Award No. 206283 (MOLINFLAM) to A. M.), the Hungarian Office for Research and Technology (Anyos Jedlik Award No. NKFP-A1-0069/2006 to A. M.), the Deutsche Forschungsgemeinschaft (SPP1468-IMMUNOBONE to G. S.), the European Union (MASTERSWITCH project to G. S.), the Norway Grants Scheme (0046/NA/2006-2/ÖP-9 to É. R.) and the University of Debrecen (OEC Mec-10/2008 Award to K. K.-T.).

### Conflict of interest

The authors declare that no financial conflict of interest exists.

### Address

Department of Physiology, Semmelweis University School of Medicine, 1094 Budapest, Hungary (Z. Kertész, D. Györi, Z. Jakus, A. Mócsai); Independent Section of Radiology, Semmelweis University, 1089 Budapest, Hungary (S. Körmendi, C. Dobó-Nagy); Department of Immunology, Medical and Health Science Center, University of Debrecen, 4032 Debrecen, Hungary (T. Fekete, K. Kis-Tóth, E. Rajnavölgyi); Department of Internal Medicine 3, University of Erlangen-Nuremberg, 91054 Erlangen, Germany (G. Schett).

**Correspondence to:** Attila Mócsai, Department of Physiology, Semmelweis University School of Medicine, PO Box 259, 1444 Budapest, Hungary. Tel.: +36-1-459-1500 Ext. 60-409; fax: +36-1-266-7480; e-mail: mocsai@eok.sote.hu

Received 10 September 2010; accepted 16 May 2011

### References

- Teitelbaum SL. Bone resorption by osteoclasts. *Science* 2000;**289**: 1504-8.
- Raggatt LJ, Partridge NC. Cellular and molecular mechanisms of bone remodeling. *J Biol Chem* 2010;**285**:25103-8.

- 3 Schett G, Teitelbaum SL. Osteoclasts and arthritis. *J Bone Miner Res* 2009;**24**:1142–6.
- 4 Teitelbaum SL. Osteoclasts: what do they do and how do they do it? *Am J Pathol* 2007;**170**:427–35.
- 5 Takayanagi H. Osteoimmunology: shared mechanisms and cross-talk between the immune and bone systems. *Nat Rev Immunol* 2007;**7**:292–304.
- 6 McInnes IB, Schett G. Cytokines in the pathogenesis of rheumatoid arthritis. *Nat Rev Immunol* 2007;**7**:429–42.
- 7 Cheng X, Kinoshita M, Murali R, Greene MI. The TNF receptor superfamily: role in immune inflammation and bone formation. *Immunol Res* 2003;**27**:287–94.
- 8 Takayanagi H. The role of NFAT in osteoclast formation. *Ann N Y Acad Sci* 2007;**1116**:227–37.
- 9 Soysa NS, Alles N. NF- $\kappa$ B functions in osteoclasts. *Biochem Biophys Res Commun* 2009;**378**:1–5.
- 10 Mócsai A, Humphrey MB, Van Ziffle JA, Hu Y, Burghardt A, Spusta SC *et al*. The immunomodulatory adapter proteins DAP12 and Fc receptor  $\gamma$ -chain (FcR $\gamma$ ) regulate development of functional osteoclasts through the Syk tyrosine kinase. *Proc Natl Acad Sci USA* 2004;**101**:6158–63.
- 11 Koga T, Inui M, Inoue K, Kim S, Suematsu A, Kobayashi E *et al*. Costimulatory signals mediated by the ITAM motif cooperate with RANKL for bone homeostasis. *Nature* 2004;**428**:758–63.
- 12 Kaifu T, Nakahara J, Inui M, Mishima K, Momiyama T, Kaji M *et al*. Osteopetrosis and thalamic hypomyelination with synaptic degeneration in DAP12-deficient mice. *J Clin Invest* 2003;**111**:323–32.
- 13 Humphrey MB, Ogasawara K, Yao W, Spusta SC, Daws MR, Lane NE *et al*. The signaling adapter protein DAP12 regulates multinucleation during osteoclast development. *J Bone Miner Res* 2004;**19**:224–34.
- 14 Faccio R, Zou W, Colaianni G, Teitelbaum SL, Ross FP. High dose M-CSF partially rescues the Dap12<sup>-/-</sup> osteoclast phenotype. *J Cell Biochem* 2003;**90**:871–83.
- 15 Mócsai A, Abram CL, Jakus Z, Hu Y, Lanier LL, Lowell CA. Integrin signaling in neutrophils and macrophages uses adaptors containing immunoreceptor tyrosine-based activation motifs. *Nat Immunol* 2006;**7**:1326–33.
- 16 Kiefer F, Brumell J, Al-Alawi N, Latour S, Cheng A, Veillette A *et al*. The Syk protein tyrosine kinase is essential for Fc $\gamma$  receptor signaling in macrophages and neutrophils. *Mol Cell Biol* 1998;**18**:4209–20.
- 17 Ji H, Ohmura K, Mahmood U, Lee DM, Hofhuis FM, Boackle SA *et al*. Arthritis critically dependent on innate immune system players. *Immunity* 2002;**16**:157–68.
- 18 Jakus Z, Németh T, Verbeek JS, Mócsai A. Critical but overlapping role of Fc $\gamma$ RIII and Fc $\gamma$ RIV in activation of murine neutrophils by immobilized immune complexes. *J Immunol* 2008;**180**:618–29.
- 19 Jakus Z, Simon E, Balázs B, Mócsai A. Genetic deficiency of Syk protects mice from autoantibody-induced arthritis. *Arthritis Rheum* 2010;**62**:1899–910.
- 20 Patterson RL, van Rossum DB, Nikolaidis N, Gill DL, Snyder SH. Phospholipase C- $\gamma$ : diverse roles in receptor-mediated calcium signaling. *Trends Biochem Sci* 2005;**30**:688–97.
- 21 Ji QS, Winnier GE, Niswender KD, Horstman D, Wisdom R, Magnuson MA *et al*. Essential role of the tyrosine kinase substrate phospholipase C- $\gamma$ 1 in mammalian growth and development. *Proc Natl Acad Sci USA* 1997;**94**:2999–3003.
- 22 Shirane M, Sawa H, Kobayashi Y, Nakano T, Kitajima K, Shinkai Y *et al*. Deficiency of phospholipase C- $\gamma$ 1 impairs renal development and hematopoiesis. *Development* 2001;**128**:5173–80.
- 23 Wang D, Feng J, Wen R, Marine JC, Sangster MY, Parganas E *et al*. Phospholipase C $\gamma$ 2 is essential in the functions of B cell and several Fc receptors. *Immunity* 2000;**13**:25–35.
- 24 Graham DB, Robertson CM, Bautista J, Mascarenhas F, Diacovo MJ, Montgrain V *et al*. Neutrophil-mediated oxidative burst and host defense are controlled by a Vav-PLC $\gamma$ 2 signaling axis in mice. *J Clin Invest* 2007;**117**:3445–52.
- 25 Cremasco V, Graham DB, Novack DV, Swat W, Faccio R. Vav/Phospholipase C $\gamma$ 2-mediated control of a neutrophil-dependent murine model of rheumatoid arthritis. *Arthritis Rheum* 2008;**58**:2712–22.
- 26 Jakus Z, Simon E, Frommhold D, Sperandio M, Mócsai A. Critical role of phospholipase C $\gamma$ 2 in integrin and Fc receptor-mediated neutrophil functions and the effector phase of autoimmune arthritis. *J Exp Med* 2009;**206**:577–93.
- 27 Watson SP, Auger JM, McCarty OJ, Pearce AC. GPVI and integrin  $\alpha$ <sub>IIb</sub> $\beta$ <sub>3</sub> signaling in platelets. *J Thromb Haemost* 2005;**3**:1752–62.
- 28 Watson SP, Herbert JM, Pollitt AY. GPVI and CLEC-2 in hemostasis and vascular integrity. *J Thromb Haemost* 2010;**8**:1456–67.
- 29 Mócsai A, Ruland J, Tybulewicz VL. The SYK tyrosine kinase: a crucial player in diverse biological functions. *Nat Rev Immunol* 2010;**10**:387–402.
- 30 Jakus Z, Fodor S, Abram CL, Lowell CA, Mócsai A. Immunoreceptor-like signaling by  $\beta$ <sub>2</sub> and  $\beta$ <sub>3</sub> integrins. *Trends Cell Biol* 2007;**17**:493–501.
- 31 Takayanagi H, Kim S, Koga T, Nishina H, Isshiki M, Yoshida H *et al*. Induction and activation of the transcription factor NFATc1 (NFAT2) integrate RANKL signaling in terminal differentiation of osteoclasts. *Dev Cell* 2002;**3**:889–901.
- 32 Bouxsein ML, Boyd SK, Christiansen BA, Guldberg RE, Jepsen KJ, Muller R. Guidelines for assessment of bone microstructure in rodents using micro-computed tomography. *J Bone Miner Res* 2010;**25**:1468–86.
- 33 Parfitt AM, Drezner MK, Glorieux FH, Kanis JA, Malluche H, Meunier PJ *et al*. Bone histomorphometry: standardization of nomenclature, symbols, and units. Report of the ASBMR Histomorphometry Nomenclature Committee. *J Bone Miner Res* 1987;**2**:595–610.
- 34 Zaiss MM, Sarter K, Hess A, Engelke K, Bohm C, Nimmerjahn F *et al*. Increased bone density and resistance to ovariectomy-induced bone loss in FoxP3-transgenic mice based on impaired osteoclast differentiation. *Arthritis Rheum* 2010;**62**:2328–38.
- 35 Takeshita S, Kaji K, Kudo A. Identification and characterization of the new osteoclast progenitor with macrophage phenotypes being able to differentiate into mature osteoclasts. *J Bone Miner Res* 2000;**15**:1477–88.
- 36 Sztatmári I, Gogolák P, Im JS, Dezsó B, Rajnavölgyi E, Nagy L. Activation of PPAR $\gamma$  specifies a dendritic cell subtype capable of enhanced induction of iNKT cell expansion. *Immunity* 2004;**21**:95–106.
- 37 Kukita T, Wada N, Kukita A, Kakimoto T, Sandra F, Toh K *et al*. RANKL-induced DC-STAMP is essential for osteoclastogenesis. *J Exp Med* 2004;**200**:941–6.
- 38 Yagi M, Miyamoto T, Sawatani Y, Iwamoto K, Hosogane N, Fujita N *et al*. DC-STAMP is essential for cell-cell fusion in osteoclasts and foreign body giant cells. *J Exp Med* 2005;**202**:345–51.
- 39 Sipos W, Pietschmann P, Rauner M, Kersch-Schindl K, Patsch J. Pathophysiology of osteoporosis. *Wien Med Wochenschr* 2009;**159**:230–4.
- 40 Kertész Z, Gyóri D, Krasznai Z, Jakus Z, Mócsai A. Role of PLC $\gamma$ 2 in osteoclasts differentiation and function. *Calcif Tissue Int* 2007;**80**:S91.

- 41 Turner M, Mee PJ, Costello PS, Williams O, Price AA, Duddy LP *et al.* Perinatal lethality and blocked B-cell development in mice lacking the tyrosine kinase Syk. *Nature* 1995;**378**:298–302.
- 42 Mao D, Epple H, Uthgenannt B, Novack DV, Faccio R. PLC $\gamma$ 2 regulates osteoclastogenesis via its interaction with ITAM proteins and GAB2. *J Clin Invest* 2006;**116**:2869–79.
- 43 Chen Y, Wang X, Di L, Fu G, Bai L, Liu J *et al.* Phospholipase C $\gamma$ 2 mediates RANKL-stimulated lymph node organogenesis and osteoclastogenesis. *J Biol Chem* 2008;**283**:29593–601.
- 44 Miyamoto T, Arai F, Ohneda O, Takagi K, Anderson DM, Suda T. An adherent condition is required for formation of multinuclear osteoclasts in the presence of macrophage colony-stimulating factor and receptor activator of nuclear factor  $\kappa$ B ligand. *Blood* 2000;**96**:4335–43.
- 45 Epple H, Cremasco V, Zhang K, Mao D, Longmore GD, Faccio R. Phospholipase C $\gamma$ 2 modulates integrin signaling in the osteoclast by affecting the localization and activation of Src kinase. *Mol Cell Biol* 2008;**28**:3610–22.
- 46 Faccio R, Takeshita S, Zallone A, Ross FP, Teitelbaum SL. c-Fms and the  $\alpha_v\beta_3$  integrin collaborate during osteoclast differentiation. *J Clin Invest* 2003;**111**:749–58.
- 47 Wu Y, Torchia J, Yao W, Lane NE, Lanier LL, Nakamura MC *et al.* Bone microenvironment specific roles of ITAM adapter signaling during bone remodeling induced by acute estrogen-deficiency. *PLoS ONE* 2007;**2**:e586.